applied sciences

MDPI

Article

PVP-Assisted Shellac Nanofiber Membrane as Highly Efficient, Eco-Friendly, Translucent Air Filter

Shanshuai Lu [1], Congling Li [1,*], Rui Liu [2] and Aifeng Lv [1,*]

[1] College of Chemistry and Chemical Engineering, Shanghai University of Engineering Science, Shanghai 201620, China; shanshuailu@sues.edu.cn
[2] Shanghai Key Lab. of D&A for Metal-Functional Materials, School of Materials Science and Engineering, Tongji University, Shanghai 201804, China; ruiliu@tongji.edu.cn
* Correspondence: conglingli@sues.edu.cn (C.L.); lvaifeng@sues.edu.cn (A.L.)

Abstract: Particulate matter (PM), composed of tiny solids and liquid droplets in polluted air, poses a serious threat to human health. Traditional air filters usually cause secondary pollution due to their poor degradability. Here, shellac, as an environmentally friendly natural organic material, was successfully applied to fabricate biodegradable air filters. Since pure shellac fiber shows poor mechanical properties and bad light transmittance, we then introduced a small amount of polyvinylpyrrolidone (PVP) in the shellac solution to prepare highly efficient air filter membranes by the electrospinning method. The prepared PVP-assisted shellac nanofiber membrane (P-Shellac FME) demonstrated improved filtration efficiencies as high as 95% and 98% for $PM_{2.5}$ and PM_{10}, respectively. The P-Shellac FME also showed good stability, with filtration efficiencies still above 90% and 95% for $PM_{2.5}$ and PM_{10} even after six hours of air filtering under high PM concentrations. The pressure drop going through the filter was only 101 Pa, which is also comparable to the value of 76 Pa obtained using commercial polypropylene nanofibers (PP nanofibers, peeled off from the surgical mask), indicating good air permeability of P-Shellac FME. Additionally, P-Shellac FME also showed the advantages of translucence, biodegradability, improved mechanical properties, and low cost. We believe that the P-Shellac FME will make a significant contribution in the application of air filtration.

Keywords: shellac; nanofiber; air filtration; electrospinning method; biodegradability; translucence

Citation: Lu, S.; Li, C.; Liu, R.; Lv, A. PVP-Assisted Shellac Nanofiber Membrane as Highly Efficient, Eco-Friendly, Translucent Air Filter. *Appl. Sci.* **2021**, *11*, 11094. https://doi.org/10.3390/app112311094

Academic Editor: Filippo Giannazzo

Received: 14 October 2021
Accepted: 20 November 2021
Published: 23 November 2021

1. Introduction

With the rapid development of our society, air pollution caused by human activities results, including from coal burning, industrial production, and vehicle emissions [1–3]. Particulate matter (PM) in the air pollution, defined as a suspended mixture of minute solid particles (comprising SO_2, NO_X, CO, heavy metals, and volatile organic compounds) and liquid droplets [4–6], seriously affects our living environments and has a great impact on human health [4,7–14]. In particular, $PM_{2.5}$ and PM_{10}, whose particle sizes are less than or equal to 2.5 μm and 10 μm, can enter the human circulation system through the respiratory tract, and cause damage to the lungs, heart, bronchus and other organs, and even lead to cancer [8,15–18]. Figure 1a shows a clear and a hazy day in a famous scenic spot in Beijing, where high PM concentration and poor visibility always appear. With the improvement of people's health consciousness, air filters are becoming quite necessary and indispensable.

Fibrous filters can be made from many materials, including cellulose, glass, polymers, ceramics, or metals, which are economical and capable of efficiently removing PM from gas streams. Many polymers, such as polyurethane (PU) [19], polyacrylonitrile (PAN) [20], poly(lactic acid) (PLA) [21], polyvinyl chloride (PVC), polystyrene (EPS) [22], etc., have been reported in fabricating nanofiber membranes used for air filtration. However, these highly corrosion-resistant materials cannot be degraded naturally, and usually require subsequent incineration treatment, causing secondary pollution in the ambient air [23,24]. Shellac, as a natural purple resin, is mainly distributed in Southeast Asia, such as Yunnan Province

of China and Thailand. Shellac is generally recognized as safe by the Food and Drug Administration (FDA), and therefore can be applied as a food additive and raw material in food coatings and film formulations, which indicates its good biodegradability [25–29]. In addition, the price is low, at only USD 20 for one kilogram. In this study, we explored the application of shellac nanofibers in air filtration. The purified shellac is a yellow powder (Figure 1b), and the molecular structure is shown in Figure 1c [30]. According to the literature, shellac is characterized by high brittleness. However, the polar–polar interaction between two polymers can overcome the brittleness when another polymer with high polarity was introduced (Figure S1) [31]. Shellac nanofibers also have bad light transmittance (Figure S2a). To take advantage of the shellac nanofibers' biodegradability and improve their mechanical properties and light transmittance, we introduced a small amount of polar polyvinylpyrrolidone (PVP) into the shellac solution, and successfully prepared a uniform PVP-assisted shellac nanofiber membrane (P-Shellac FME) on a metal mesh (150 mesh) using electrospinning technology. The filtration efficiencies of $PM_{2.5}$ and PM_{10} for P-Shellac were 95% and 98.1%, respectively, which is 35–40% higher than that the efficiencies of a surgical mask. In a word, the P-Shellac FME is an efficient, biodegradable, translucent, breathable air filter and has potential application prospect.

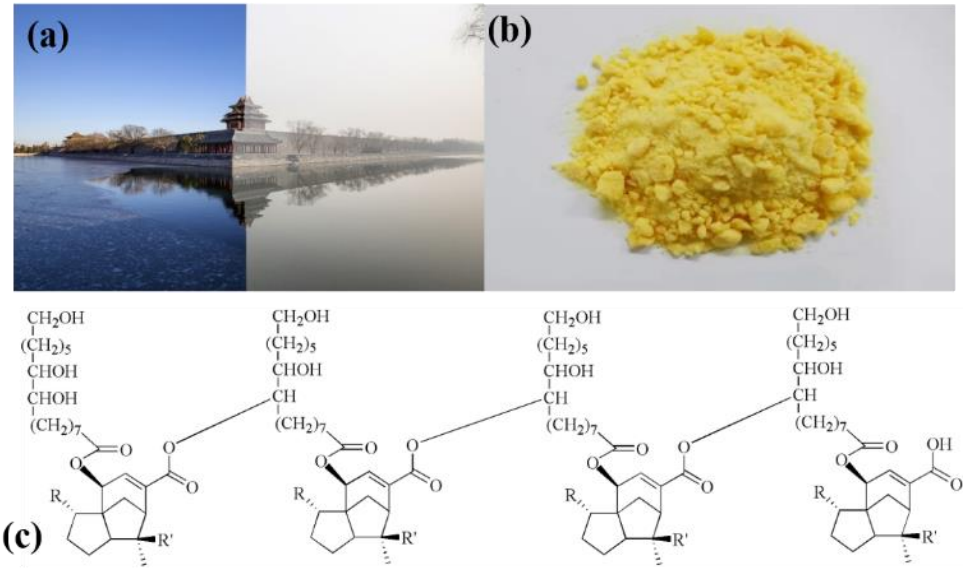

Figure 1. (**a**) A photo of a famous scenic spot in Beijing, which shows a clear and a hazy day on the left and right, respectively. (**b**) Refined shellac powder. (**c**) The chemical structure of shellac (R = CHO/COOH/CH_2OH/CH_3; R′ = CH_2OH/CH_3).

2. Materials and Methods

2.1. Materials

Shellac (99% refined bleached dewaxed shellac, food grade) was obtained from the Chu Xiong Des Shellac Co. Ltd. (Yunnan, China), which meets the Chinese standard GB-2760. PVP (M.W. = 1,300,000 g/mol), was bought from Shanghai Aladdin Bio-Chem Technology Co. Ltd. Polypropylene nanofiber membrane (PP FME) was peeled off from a surgical mask, which we bought from a supermarket. Ethanol (anhydrous, 99.7%) was obtained from Shanghai Titan Scientific Co. Ltd. All chemicals were used without further purification.

2.2. Preparation of Shellac/PVP/P-Shellac Solution

Firstly, shellac and PVP powder were separately dissolved in ethanol to prepare shellac (40% *w*/*w*) and PVP (8% *w*/*w*) solutions. Secondly, P-Shellac solution was prepared through mixing the two solutions by a weight ratio of 3:1 (40% *w*/*w* shellac to 8% *w*/*w* PVP). Thirdly, the mixed solution was stirred at 50 °C for 12 h to achieve a uniform P-Shellac solution.

2.3. Equipment for Measurement and Characterization

The concentration of PM was tested using a Dust analyzer (PGM-300 KREVOR, China), and the pressure drop (ΔP) before and after the air filter was measured by an electronic pressure meter (SD20 SUMMIT, Korea). The morphology of the nanofiber membrane was characterized by scanning electron microscopy (S-8010, Hitachi, Japan). Nano Measurer software was used to estimate the diameter distribution for 100 randomly selected nanofibers for each type of FME. Fourier Transform Infrared spectroscopy (FTIR) was performed by using a Nicolet IS50 instrument (Thermal Fisher Scientific Inc., Madison, USA).

3. Results

The prepared solutions were filled into a 5 mL syringe with a feeding rate of 1.0 mL/h. The applied voltage on the syringe was 15 kV and the distance between syringe tip and the collector was 13 cm. The nanofiber membranes were then collected on a stainless-steel mesh (150 mesh), as shown in Figure 2. The time for electrospinning was 10 min for each kind of FME. The temperature was maintained at 25 °C and the relative humidity was controlled at 40–60%.

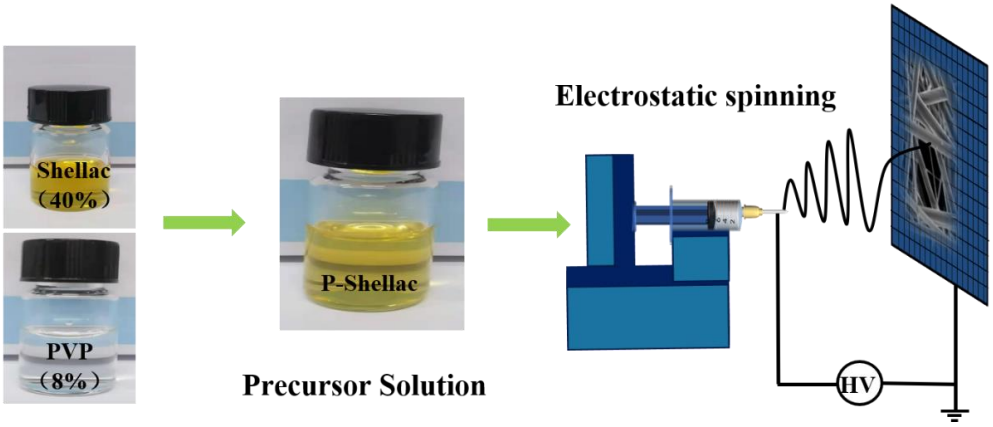

Figure 2. Schematic diagram for fabricating P-Shellac air filter by electrospinning method.

Figure 3a–c show the scanning electron microscopy (SEM) and diameter statistics of nanofibers fabricated from pure shellac, pure PVP and P-Shellac, respectively. The pure shellac nanofibers exhibited rough edges and a broad diameter distribution with the range of 400–1000 nm with a mean diameter of around 650 nm (Figure 3a), while PVP nanofibers had a smooth surface and a more uniform diameter in the range of 250–350 nm with a mean diameter of around 270 nm (Figure 3b). In comparison to pure shellac nanofibers, P-Shellac nanofibers possessed a smoother surface and a more uniform diameter, mainly (about 73%) distributed in the range of 200–500 nm with a mean diameter of around 439 nm (Figure 3c). The standard deviations of the mean diameters at different positions in the FME were less than 10 nm for all the three FME. The P-Shellac FME became translucent, while the shellac FME exhibited a white color (Figure S2). At the same time, the mechanical properties of P-Shellac nanofibers were obviously improved, as indicated by the tensile stress–strain curves (Figure S3). When we drew lines on the surface of the nanofiber membranes with tweezers, there was a clean scratch on the P-Shellac FME, but much shellac powder could be seen on the pure shellac FME (Figure S1).

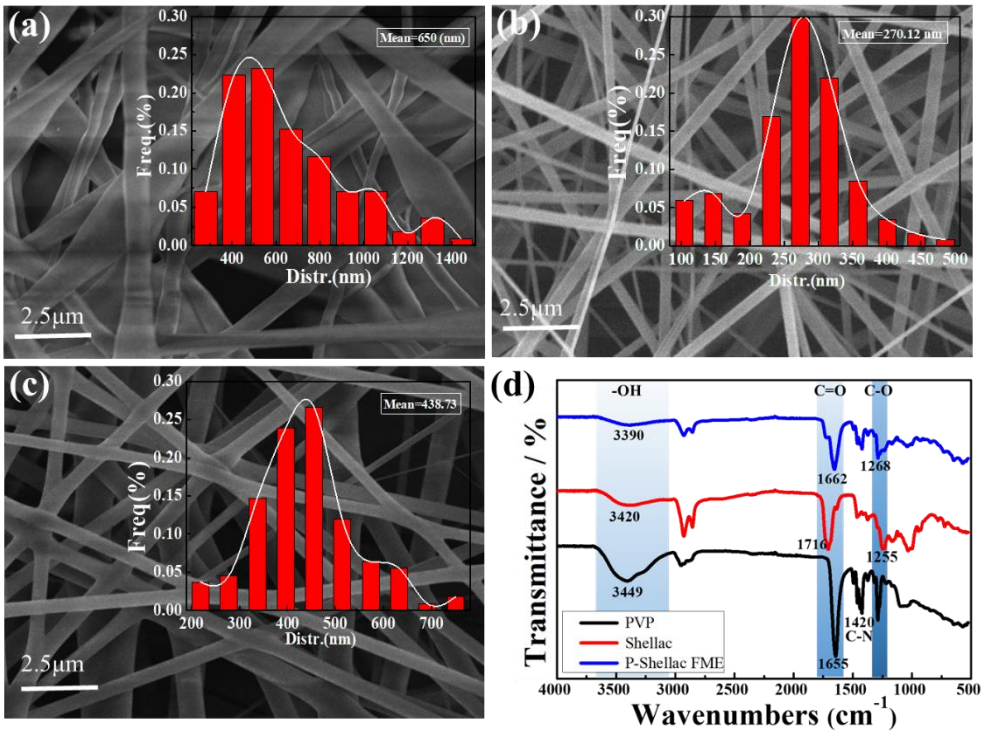

Figure 3. SEM images of nanofibers made from pure shellac (**a**), pure PVP (**b**), and P-Shellac (**c**). The insets in (**a**–**c**) are the diameter statistics of the nanofibers. (**d**) FTIR of three kinds of nanofibers.

The results of the FTIR characterization of pure shellac nanofibers, pure PVP nanofibers, and P-Shellac nanofibers are shown in Figure 3d. Firstly, for pure shellac nanofibers, the peaks at 3420 cm^{-1}, 1716 cm^{-1}, and 1255 cm^{-1} were due to -OH, C=O and C-O stretching vibration, respectively. For pure PVP nanofibers, the characteristic peaks appearing at around 3449 cm^{-1} were ascribed to the -OH stretching vibration [32], while stronger absorption peaks at 1655 cm^{-1}, 1420 cm^{-1} were ascribed to C=O and C-N stretching vibration, respectively. Compared with pure shellac, the mechanical properties of P-Shellac nanofibers were greatly improved, owing to the hydrogen bond formed between PVP (-OH, C-N and C=O) and shellac (C=O, C-O, -OH), as shown in Figure S1. The addition of PVP in the P-shellac nanofibers should contribute to improved surface smoothness, diameter distribution, and mechanical properties.

There is a clear effect of air filtration for P-Shellac FME, as shown in Figure 4. Two transparent bottles were put together mouth to mouth, with P-Shellac FME between the two bottles. PM fog was collected from burning incense, whose particle size, chemical composition including CO, NO_2, SO_2, and organic compounds attached to the PM were quite similar to those found on hazy days [33]. The top bottle was filled with PM fog, while there was only clean air in the bottom bottle. After 20 min, the bottom bottle with P-Shellac FME was still clear, and the PM fog remained only in the upper bottle (Figure 4a). By contrast, the bottom bottle without P-Shellac FME became foggy (Figure 4b). The translucent P-Shellac FME turned yellow after PM filtration (Figure 4c,d), indicating its good filtration efficiency. We found that P-Shellac FME has quite good hydrophilicity with a water contact angle of only 13 degrees (Figure S4), which is between PVP (10.7 degrees) and shellac (22 degrees). Hence, the wettability of nanofiber membrane is good and the air pollutants easily spread on the nanofibers, which could be one of the reasons for high filtration efficiency [34,35].

Figure 4. A simple filtration setup with (**a**) and without (**b**) P-Shellac FME between the top and bottom bottles. The top bottle was filled with PM fog. Optical images of P-Shellac FME before (**c**) and after (**d**) PM filtration.

To exactly evaluate air filtration efficiency, we designed a setup especially for air filtration in our lab as shown in Figure 5a. Polluted air (mainly $PM_{2.5}$ and PM_{10}) was produced by burning incense in a closed acrylic box. Suction pump and dust analyzer (PGM) was used to control the rate of air flow and measure the concentration of PM, respectively. Dust analyzer 1 (PGM-1) was connected to collection bottle 1 (CB1′) with unfiltered air, while dust analyzer 2 (PGM-2) was connected to collection bottle 2 (CB2) filled with filtered air. Filtration efficiency was calculated according to the following equation:

$$E(\%) = \frac{C_{\mathrm{PGM-2}}}{C_{\mathrm{PGM-1}}} \times 100 \quad (1)$$

where $C_{\mathrm{PGM\text{-}2}}$ is the concentration of $PM_{2.5}$ and PM_{10} measured by PGM-2, and $C_{\mathrm{PGM\text{-}1}}$ is the concentration of $PM_{2.5}$ and PM_{10} measured by PGM-1. We first measured the concentration of PM in collection bottle 1 (CB1′) after incense burning for 6 h. In addition, the average concentrations of $PM_{2.5}$ and PM_{10} of PM fog were 2150 $\mu g/m^3$ and 5600 $\mu g/m^3$, respectively (Figure S5). We then measured the concentrations of $PM_{2.5}$ and PM_{10} in collection bottle 2 after air filtration lasting 3 h. The filtration efficiency of commercial PP was also introduced for comparison.

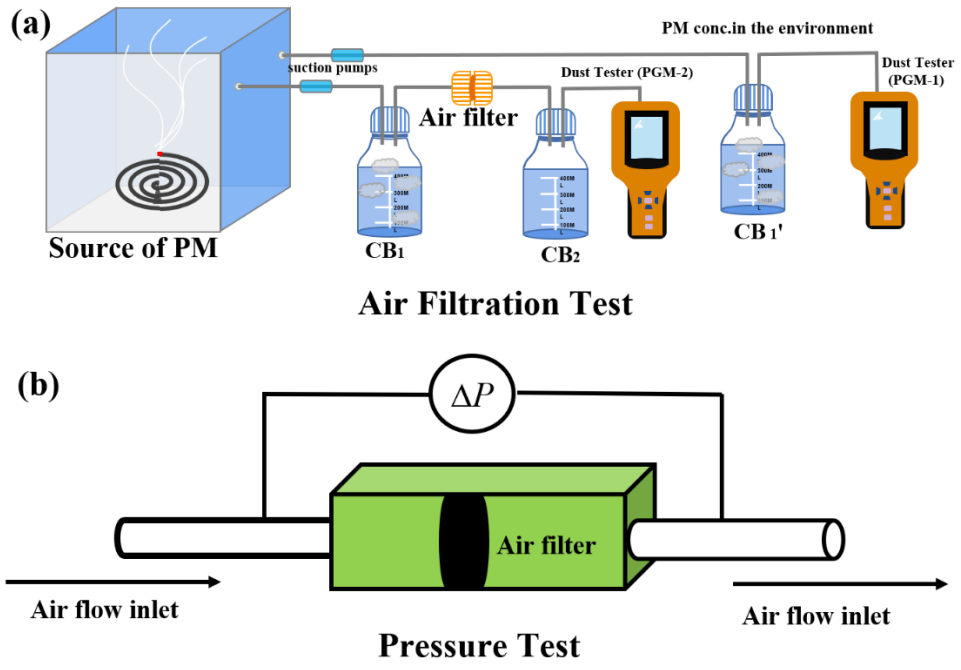

Figure 5. (**a**) Schematic of air filter setup and (**b**) pressure drop measurement.

The filtration efficiencies of $PM_{2.5}$ for FMEs made from PVP, shellac, P-Shellac and PP were 73%, 93.1%, 95% and 55.2%, respectively. The filtration efficiencies of PM_{10} for FMEs

made from PVP, shellac, P-Shellac and PP were 84.5%, 96.3%, 98.1% and 72.7%, respectively. Among the four kinds of nanofiber membranes, P-Shellac FME gave the highest filtration efficiency for both $PM_{2.5}$ and PM_{10}, much higher than PP and PVP, and a little higher than shellac (Figure 6a, Table 1). The nanofiber structure of P-Shellac and pure shellac with varying diameters should be the main reason for the high filtration performance, in which the large-diameter nanofibers with large pores play a supporting role, and they will be further divided into smaller pores by small-diameter nanofibers. The BET analysis showed that P-Shellac FME have the largest surface area, at 67.9 m^2/g, and the most mesoporous structure, much higher than the other two FMEs (Table S1 and Figure S6). The hierarchical pore structure thus could improve the filtration efficiency, delay PM aggregation, and finally result in a large pollutant carrying capacity.

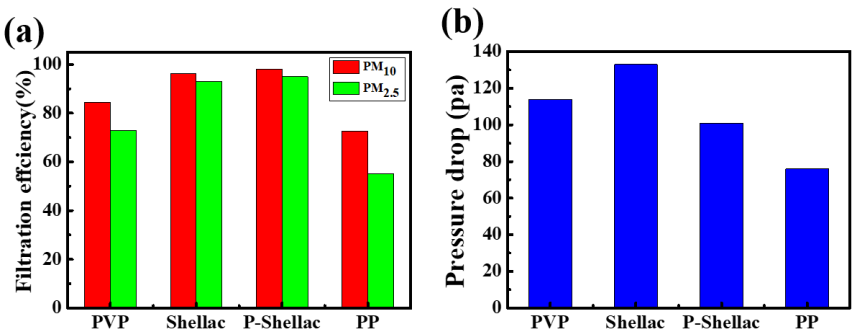

Figure 6. (**a**) Filtration efficiency and (**b**) pressure drop of four nanofiber filters. In particular, PP is peeled off from a surgical mask.

Table 1. Performance summary of air filters.

Air Filter	$E_{PM2.5}$ (%)	E_{PM10} (%)	ΔP (Pa)	$QF_{PM2.5}$ (Pa^{-1})	QF_{PM10} (Pa^{-1})
PVP	73	84.5	114	0.0115	0.016
Shellac	93.1	96.3	133	0.0201	0.0247
P-Shellac	95	98.1	101	0.029	0.0392
PP (commercial)	55.2	72.7	76	0.01	0.0171

E = PM filtration efficiency; ΔP = pressure drop; QF = quality factor.

Besides filtration efficiency, air permeability is another important feature for air filters. Pressure drop measurement was then carried out as demonstrated in Figure 5b. At an air flow rate of 0.25 m/s, the pressure drops (ΔP) of FMEs for PVP, shellac, P-Shellac and PP were measured to be 114 Pa, 133 Pa, 101 Pa and 76 Pa, respectively (Figure 6b), which exhibited only 0.11%, 0.13%, 0.1% and 0.07% pressure drops with reference to atmospheric pressure (101,325 Pa). It was found that all the three FMEs have comparable air permeability to commercial filter PP. The filtration performance of FME is evaluated by a quality factor (QF) [36], which is defined as:

$$QF = \frac{-\ln(1-E)}{\Delta P} \quad (2)$$

where E is the filtration efficiency of PM and ΔP represents the pressure drop. P-Shellac FME showed much higher QF (Pa^{-1}) for $PM_{2.5}$ and PM_{10} (0.029, 0.0392) than that of PVP (0.0115, 0.016) and shellac FME (0.0201, 0.0247), which indicates that the hydrogen bond formed in the mixture P-Shellac could improve the filter performance (Table 1). The QFs of $PM_{2.5}$ and PM_{10} for FEMs fabricated from PVP, shellac and P-Shellac were all higher than that of the commercial PP air filters (0.01, 0.0171).

4. Discussion

We then investigated the filtration mechanism of P-Shellac FME (Figure 7). To explore the filtration process in the FEM, the PM filtration by P-Shellac nanofibers at different times (0 h, 0.5 h, 1 h, 2 h, 3 h, 6 h) was characterized by SEM. Before air filtration started, the surface and edge of the P-Shellac nanofibers were smooth (Figure 7a). PM particles were

randomly captured and adhered tightly to the nanofiber surface when polluted air flowed through the P-Shellac nanofiber network (Figure 7b,c). While the air filtration was taking place, PM particles gradually aggregated (Figure 7d), wrapped (Figure 7e), and diffused uniformly (Figure 7f) on the surface of nanofibers. The nanofiber surface became smooth again, although the diameter increased, which maintained the interspace of nanofibers and caused them to still possess good air permeability after 6 h of air filtration (Figure 7g). We also studied the reasons for the induction of interception and deposition of PM. In view of the molecular structure of P-Shellac, there are large quantities of hydroxyl and ester groups in shellac and larger dipole moment (around 2.3 D) in PVP [37]. The generated strong dipole–dipole and induced-dipole intermolecular forces could obviously increase the adsorption ability of P-Shellac FME [38]. FTIR characterization of three FMEs after air filtration showed that each of the three -OH, C=O and C-O stretching vibrations became weak, indicating the existence of an interaction between PM and nanofiber membranes (Figure S7).

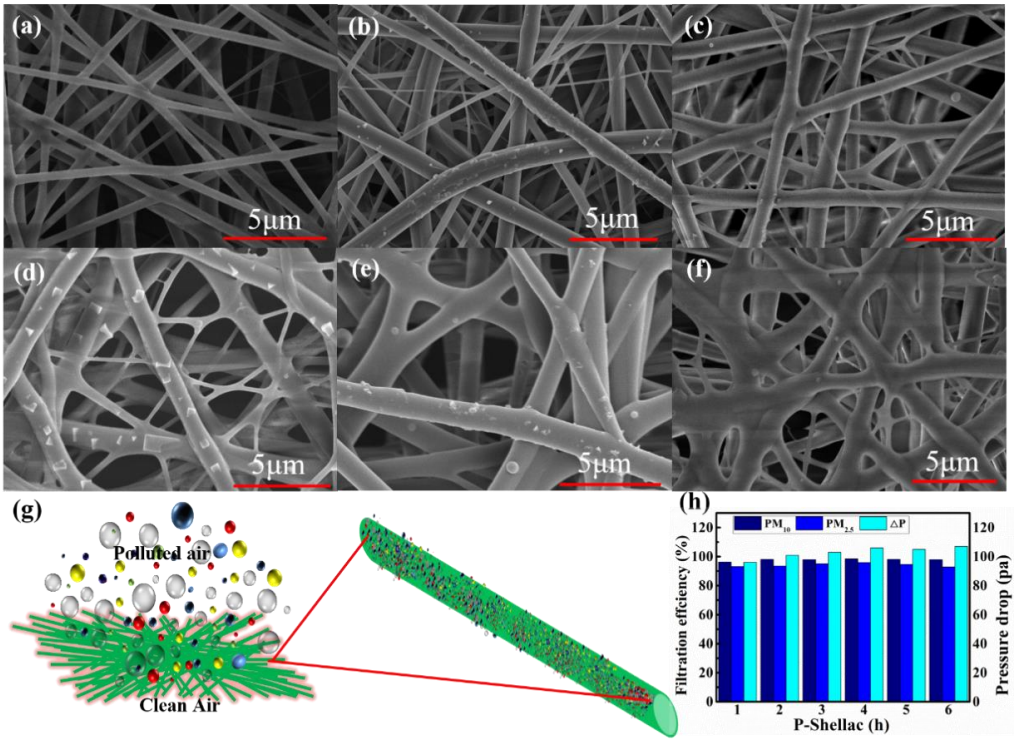

Figure 7. (**a**–**f**) SEM images of P-Shellac nanofiber membranes under a continuous flow of smoke at different times (0 h, 0.5 h, 1 h, 2 h, 3 h and 6 h). (**g**) Schematic diagram of the air filtration and aggregation of PM particles on P-Shellac FME. (**h**) Filtration efficiency and pressure drop for P-Shellac FME filtered at different times.

The filtration efficiency and air permeability of P-Shellac FME has good long-term stability (Figure 7h). Under high PM concentrations, air filtration lasted continuous six hours, the filtration efficiency of $PM_{2.5}$ and PM_{10} could still be maintained at above 90% and 95%, respectively. Moreover, the pressure drop presented negligible change, implying that the P-Shellac FME could keep good air permeability even under long-term and high-concentration PM filtration. Hence, P-Shellac FME showed superior comprehensive performance as an air filter.

5. Conclusions

In summary, we successfully fabricated P-Shellac FME by a facile electrospinning method. The obtained P-Shellac FME exhibited excellent filtration performance for both $PM_{2.5}$ and PM_{10}, and was much higher than that of commercial materials. Owing to its special chemical structure, P-Shellac FME not only showed high filtration efficiency up to

95% and 98% for $PM_{2.5}$ and PM_{10}, but also possessed decent air permeability and translucence. Moreover, P-Shellac FME has the characteristic of biodegradability, avoiding the secondary pollution during the decomposing process of traditional nanofiber filters. We believe that the high filtration performance, good air permeability, nice stability, translucence, biodegradability and low price of shellac give the P-Shellac FME great potential in real applications.

Supplementary Materials: The following are available online at https://www.mdpi.com/article/10.3390/app112311094/s1, Figure S1: Optical images of P-shellac FME and shellac fiber membrane scratched by a tweezer, Figure S2: Optical images of pure shellac nanofiber membrane and translucent P-Shellac FME, Figure S3: The tensile stress–strain curves, Figure S4: Contact angles, Figure S5: The concentrations of PM_{10} and $PM_{2.5}$ in CB1′, Figure S6: BET analysis, Table S1: BET analysis summary, Figure S7: FTIR of three FMEs after air filtration.

Author Contributions: Conceptualization, A.L.; methodology, S.L.; software, S.L.; validation, R.L.; formal analysis, C.L.; investigation, S.L. and C.L.; resources, A.L.; data curation, S.L. and C.L.; writing—original draft preparation, S.L. and C.L.; writing—review and editing, A.L.; visualization, A.L. and R.L.; supervision, A.L.; project administration, A.L.; funding acquisition, A.L. All authors have read and agreed to the published version of the manuscript.

Funding: This research was funded by the National Natural Science Foundation of China (51803118, 22008150) and the Program for Professor of Special Appointment (Eastern Scholar) at Shanghai Institutions of Higher Learning.

Institutional Review Board Statement: Not applicable.

Informed Consent Statement: Not applicable.

Data Availability Statement: Not applicable.

Acknowledgments: We acknowledge the support from the Shanghai University of Engineering Science.

Conflicts of Interest: The authors declare no conflict of interest.

References

1. Tian, Y.; Liu, X.; Huo, R.; Shi, Z.; Sun, Y.; Feng, Y.; Harrison, R.M. Organic compound source profiles of $PM_{2.5}$ from traffic emissions, coal combustion, industrial processes and dust. *Chemosphere* **2021**, *278*, 130429. [CrossRef] [PubMed]
2. Park, S.S.; Kim, Y.J. Source contributions to fine particulate matter in an urban atmosphere. *Chemosphere* **2005**, *59*, 217–226. [CrossRef]
3. Zhang, Q.; Jiang, X.; Tong, D.; Davis, S.J.; Zhao, H.; Geng, G.; Feng, T.; Zheng, B.; Lu, Z.; Streets, D.G.; et al. Transboundary health impacts of transported global air pollution and international trade. *Nature* **2017**, *543*, 705–709. [CrossRef] [PubMed]
4. Martins, N.R.; Carrilho da Graça, G. Impact of $PM_{2.5}$ in indoor urban environments: A review. *Sustain. Cities Soc.* **2018**, *42*, 259–275. [CrossRef]
5. Li, F.; Yan, J.; Wei, Y.; Zeng, J.; Wang, X.; Chen, X.; Zhang, C.; Li, W.; Chen, M.; Lü, G. $PM_{2.5}$-bound heavy metals from the major cities in China: Spatiotemporal distribution, fuzzy exposure assessment and health risk management. *J. Clean. Prod.* **2021**, *286*, 124967. [CrossRef]
6. Li, Y.; Liao, Q.; Zhao, X.; Tao, Y.; Bai, Y.; Lu, P. Premature mortality attributable to $PM_{2.5}$ pollution in China during 2008–2016: Underlying causes and responses to emission reductions. *Chemosphere* **2021**, *263*, 127925. [CrossRef] [PubMed]
7. Morelli, X.; Rieux, C.; Cyrys, J.; Forsberg, B.; Slama, R. Air pollution, health and social deprivation: A fine-scale risk assessment. *Environ. Res.* **2016**, *147*, 59–70. [CrossRef] [PubMed]
8. Raaschou-Nielsen, O.; Andersen, Z.J.; Beelen, R.; Samoli, E.; Stafoggia, M.; Weinmayr, G.; Hoffmann, B.; Fischer, P.; Nieuwenhuijsen, M.J.; Brunekreef, B.; et al. Air pollution and lung cancer incidence in 17 European cohorts: Prospective analyses from the European study of cohorts for air pollution effects (ESCAPE). *Lancet Oncol.* **2013**, *14*, 813–822. [CrossRef]
9. Shang, Y.; Sun, Z.; Cao, J.; Wang, X.; Zhong, L.; Bi, X.; Li, H.; Liu, W.; Zhu, T.; Huang, W. Systematic review of Chinese studies of short-term exposure to air pollution and daily mortality. *Environ. Int.* **2013**, *54*, 100–111. [CrossRef]
10. Loomis, D.; Grosse, Y.; Lauby-Secretan, B.; Ghissassi, F.E.; Bouvard, V.; Benbrahim-Tallaa, L.; Guha, N.; Baan, R.; Mattock, H.; Straif, K. The carcinogenicity of outdoor air pollution. *Lancet Oncol.* **2013**, *14*, 1262–1263. [CrossRef]
11. Beelen, R.; Raaschou-Nielsen, O.; Stafoggia, M.; Andersen, Z.J.; Weinmayr, G.; Hoffmann, B.; Wolf, K.; Samoli, E.; Fischer, P.; Nieuwenhuijsen, M.; et al. Effects of long-term exposure to air pollution on natural-cause mortality: An analysis of 22 European cohorts within the multicentre ESCAPE project. *Lancet* **2014**, *383*, 785–795. [CrossRef]
12. Nel, A. Atmosphere. Air pollution-related illness: Effects of particles. *Science* **2005**, *308*, 804–806. [CrossRef] [PubMed]

13. Lelieveld, J.; Evans, J.S.; Fnais, M.; Giannadaki, D.; Pozzer, A. The contribution of outdoor air pollution sources to premature mortality on a global scale. *Nature* **2015**, *525*, 367–371. [CrossRef] [PubMed]
14. Cole-Hunter, T.; Dhingra, R.; Fedak, K.M.; Good, N.; L'Orange, C.; Luckasen, G.; Mehaffy, J.; Walker, E.; Wilson, A.; Balmes, J.; et al. Short-term differences in cardiac function following controlled exposure to cookstove air pollution: The subclinical tests on volunteers exposed to smoke (STOVES) study. *Environ. Int.* **2021**, *146*, 106254. [CrossRef]
15. Pope III, C.A.; Burnett, R.T.; Thun, M.J.; Calle, E.E.; Krewski, D.; Ito, K.; Thurston, G.D. Lung Cancer, Cardiopulmonary Mortality, and Long-term Exposure to Fine Particulate Air Pollution. *JAMA* **2002**, *287*, 1132–1141. [CrossRef]
16. Wang, G.; Huang, L.; Gao, S.; Gao, S.; Wang, L. Measurements of PM_{10} and $PM_{2.5}$ in urban area of Nanjing, China and the assessment of pulmonary deposition of particle mass. *Chemosphere* **2002**, *48*, 689–695. [CrossRef]
17. Yang, L.; Shang, Y.; Hannigan, M.P.; Zhu, R.; Wang, Q.g.; Qin, C.; Xie, M. Collocated speciation of $PM_{2.5}$ using tandem quartz filters in northern nanjing, China: Sampling artifacts and measurement uncertainty. *Atmos. Environ.* **2021**, *246*, 118066. [CrossRef]
18. Barkjohn, K.K.; Bergin, M.H.; Norris, C.; Schauer, J.J.; Zhang, Y.; Black, M.; Hu, M.; Zhang, J. Using Low-cost sensors to Quantify the Effects of Air Filtration on Indoor and Personal Exposure Relevant $PM_{2.5}$ Concentrations in Beijing, China. *Aerosol Air Qual. Res.* **2020**, *20*, 297–313. [CrossRef]
19. Liu, F.; Li, M.; Shao, W.; Yue, W.; Hu, B.; Weng, K.; Chen, Y.; Liao, X.; He, J. Preparation of a polyurethane electret nanofiber membrane and its air-filtration performance. *J. Colloid Interf. Sci.* **2019**, *557*, 318–327. [CrossRef]
20. Wang, N.; Si, Y.; Wang, N.; Sun, G.; El-Newehy, M.; Al-Deyab, S.S.; Ding, B. Multilevel structured polyacrylonitrile/silica nanofibrous membranes for high-performance air filtration. *Sep. Purif. Technol.* **2014**, *126*, 44–51. [CrossRef]
21. Wang, Z.; Zhao, C.; Pan, Z. Porous bead-on-string poly(lactic acid) fibrous membranes for air filtration. *J. Colloid Interf. Sci.* **2015**, *441*, 121–129. [CrossRef]
22. Rajak, A.; Hapidin, D.A.; Iskandar, F.; Munir, M.M.; Khairurrijal, K. Electrospun nanofiber from various source of expanded polystyrene (EPS) waste and their characterization as potential air filter media. *Waste Manag.* **2020**, *103*, 76–86. [CrossRef]
23. Geyer, G.; Jambeck, J.R.; Lavender Law, K. Production, use, and fate of all plastics ever made. *Sci. Adv.* **2017**, *3*, e1700782. [CrossRef]
24. Webb, H.; Arnott, J.; Crawford, R.; Ivanova, E. Plastic degradation and its environmental implications with special reference to poly(ethylene terephthalate). *Polymers* **2012**, *5*, 1–18. [CrossRef]
25. Mauri, S.; Okamoto, Y. Final report on the safety assessment of shellac. *J. Am. Coll. Toxicol.* **1986**, *5*, 309–327.
26. Ghoshal, S.; Khan, M.A.; Khan, R.A.; Gul-E-Noor, F.; Sarwaruddin Chowdhury, A.M. Study on the Thermo-Mechanical and Biodegradable Properties of Shellac Films Grafted with Acrylic Monomers by Gamma Radiation. *J. Polym. Environ.* **2010**, *18*, 216–223. [CrossRef]
27. Qin, O.; Cheng, Y.; Hu, W.; Zhou, H.; Tan, Y.; Guo, S.; Jin, X.; Tao, L.; Du, L.; Wang, J.; et al. Patch test in Chinese in Shanghai with cosmetic allergy to cosmetic series and products. *J. Cosmet Dermatol-US* **2020**, *19*, 2086–2092. [CrossRef]
28. Yuan, Y.; He, N.; Xue, Q.; Guo, Q.; Dong, L.; Haruna, M.H.; Zhang, X.; Li, B.; Li, L. Shellac: A promising natural polymer in the food industry. *Trends Food Sci. Tech.* **2021**, *109*, 139–153. [CrossRef]
29. Wang, X.; Yu, D.-G.; Li, X.-Y.; Bligh, S.W.A.; Williams, G.R. Electrospun medicated shellac nanofibers for colon-targeted drug delivery. *Int. J. Pharmaceut.* **2015**, *490*, 384–390. [CrossRef] [PubMed]
30. Wang, L.; Ishida, Y.; Ohtani, H.; Tsuge, S.; Nakayama, T. Characterization of natural resin shellac by reactive pyrolysis-gas chromatography in the presence of organic alkali. *Anal. Chem.* **1999**, *71*, 1316–1322. [CrossRef] [PubMed]
31. Wang, R.; An, N.; Feng, W.; Zhang, H.; Wang, T. Antibacterial Fresh-Keeping Films Assembled by Synergistic Interplay Between Casein and Shellac. *Food Biophys.* **2021**. [CrossRef]
32. Koczkur, K.M.; Mourdikoudis, S.; Polavarapu, L.; Skrabalak, S.E. Polyvinylpyrrolidone (PVP) in nanoparticle synthesis. *Dalton Trans.* **2015**, *44*, 17883–17905. [CrossRef]
33. Lin, T.-C.; Krishnaswamy, G.; Chi, D.S. Incense smoke: Clinical, structural and molecular effects on airway disease. *Clin. Mol. Allergy* **2008**, *6*, 3. [CrossRef]
34. Gao, X.; Gou, J.; Zhang, L.; Duan, S.; Li, C. A silk fibroin based green nano-filter for air filtration. *RSC Adv.* **2018**, *8*, 8181–8189. [CrossRef]
35. Gao, X.; Wen, S.; Yang, B.; Xue, J.; Wang, H. Enhanced air filtration performance under high-humidity condition through electrospun membranes with optimized structure. *Chin. J. Chem. Eng.* **2020**, *28*, 1788–1795. [CrossRef]
36. Min, K.; Kim, S.; Kim, S. Silk protein nanofibers for highly efficient, eco-friendly, optically translucent, and multifunctional air filters. *Sci. Rep.* **2018**, *8*, 9598. [CrossRef] [PubMed]
37. Liu, C.; Hsu, P.-C.; Lee, H.-W.; Ye, M.; Zheng, G.; Liu, N.; Li, W.; Cui, Y. Transparent air filter for high-efficiency $PM_{2.5}$ capture. *Nat. Commun.* **2015**, *6*, 6205. [CrossRef] [PubMed]
38. Xiao, J.; Liang, J.; Zhang, C.; Tao, Y.; Ling, G.-W.; Yang, Q.-H. Advanced materials for capturing particulate matter: Progress and perspectives. *Small Methods* **2018**, *2*, 1800012.